Inorganic Chemistry

Article

pubs.acs.org/IC

Ion Association in $AlCl_3$ Aqueous Solutions from Constrained First-Principles Molecular Dynamics

Emilie Cauët,*[,†,‡,§] Stuart A. Bogatko,[†,⊥,§] Eric J. Bylaska,[∥] and John H. Weare[†]

[†]Department of Chemistry and Biochemistry, University of California, San Diego, La Jolla, California 92093, United States

[∥]Pacific Northwest National Laboratory, P.O. Box 999, Richland, Washington 99352, United States

Supporting Information

ABSTRACT: The Car−Parrinello-based molecular dynamics (CPMD) method was used to investigate the ion-pairing behavior between Cl^- and Al^{3+} ions in an aqueous $AlCl_3$ solution containing 63 water molecules. A series of constrained simulations was carried out at 300 K for up to 16 ps each, with the internuclear separation (r_{Al-Cl}) between the Al^{3+} ion and one of the Cl^- ions held constant. The calculated potential of mean force (PMF) of the Al^{3+}−Cl^- ion pair shows a global minimum at r_{Al-Cl} = 2.3 Å corresponding to a contact ion pair (CIP). Two local minima assigned to solvent-separated ion pairs (SSIPs) are identified at r_{Al-Cl} = 4.4 and 6.0 Å. The positions of the free energy minima coincide with the hydration-shell intervals of the Al^{3+} cation, suggesting that the Cl^- ion is inclined to reside in regions with low concentrations of water molecules, that is, between the first and second hydration shells of Al^{3+} and between the second shell and the bulk. A detailed analysis of the solvent structure around the Al^{3+} and Cl^- ions as a function of r_{Al-Cl} is presented. The results are compared to structural data from X-ray measurements and unconstrained CPMD simulations of single Al^{3+} and Cl^- ions and $AlCl_3$ solutions. The dipole moments of the water molecules in the first and second hydration shells of Al^{3+} and in the bulk region and those of Cl^- ions were calculated as a function of r_{Al-Cl}. Major changes in the electronic structure of the system were found to result from the removal of Cl^- from the first hydration shell of the Al^{3+} cation. Finally, two unconstrained CPMD simulations of aqueous $AlCl_3$ solutions corresponding to CIP and SSIP configurations were performed (17 ps, 300 K). Only minor structural changes were observed in these systems, confirming their stability.

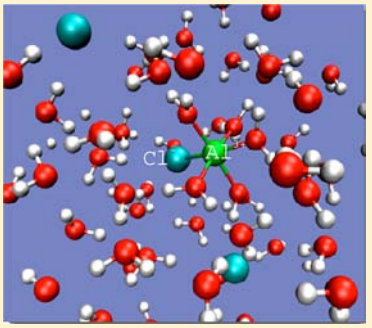

1. INTRODUCTION

Aluminum, the third most abundant element in Earth's crust, is a key component in the important aluminum silicate minerals. As a product of the dissolution of these minerals upon contact with acid waters (e.g., acid rain), the Al^{3+} cation is a major hazardous species in natural waters,[1] whereas the most common anion (highest concentration) in most natural waters is the chloride ion. The Al^{3+} cation exists, in solution, as a variety of oxohydroxo ion species (some of which are polyion species) that have been intensively studied for many years.[2−10] Small aqueous aluminum species and clusters have been characterized and used as models to determine reaction rates and pathways at the molecular scale. The kinetics of water-exchange reactions in aluminum has been extensively investigated both spectroscopically (using mostly NMR measurements)[1,7,11−18] and theoretically (ab initio and molecular dynamics calculations).[18−23] The influence of important bound ligands such as fluorine has also been investigated, mostly on the rate of water exchange for Al^{3+}.[11,19,24,25] Although the interaction of Al^{3+} cationic metal species with Cl^- anions plays a key role in the transport of many metal species in aqueous environments, it still remains unclear whether Cl^- ion and Al^{3+} metal ion tend to associate. The structural role of the Cl^- anion in the hydration shells of the Al^{3+} cation is still not well understood, and many aspects, such as how the solvent structures itself as the two ions approach each other, still require further study.

Spectroscopic measurements[26−28] (mostly by UV−vis, IR, Raman, and NMR spectroscopies) and relaxation methods[29] such as dielectric or ultrasonic relaxation have generally played a significant role in the elucidation of ion-association phenomena[30] by providing valuable insights into the nature and kinetics of ion pairs. Although it is widely assumed that simple 3:1 chloride electrolytes (e.g., $AlCl_3$, $FeCl_3$) are completely dissociated and free in dilute aqueous solutions, there are indications that, for some systems, the Cl^- ions are bound to the trivalent metal cations. Indeed, X-ray absorption spectroscopy (XAS) experiments[31] suggest the presence of chloro ligands in the inner solvation sphere of Fe^{3+} and Cr^{3+}, whereas no experimental evidence of chloro ligand has been reported for Al^{3+}. According to ref 31, the results can be interpreted in terms of the electronic structure of the solvated trivalent metal ion. In this regard, extended X-ray absorption fine structure (EXAFS) experiments[32] have been performed to investigate the structures of the inner and outer spheres of chloroaquo complexes of Cr^{3+} in aqueous solutions. Sarpola et al. studied aluminum(III)[33,34] and iron(III)[35] solutions with electrospray ionization time-of-flight mass spectrometry (ESI-

Received: June 25, 2012
Published: October 4, 2012

   dx.doi.org/10.1021/ic301346k | *Inorg. Chem.* 2012, 51, 10856−10869

ToF MS) as a function of time. These experiments, in which the complexes were dehydrated before they entered the mass spectrometer, provide evidence for the presence of a variety of monomeric and polymeric complexes ranging from Fe_1 to Fe_4 and from Al_1 to Al_{32} cores for Fe^{3+} and Al^{3+}, respectively, with different numbers of hydroxo as well as chloro ligands. Although the existence of chlorido-bridged structures was reported only for large Fe(III) complexes, the authors showed that, in most small Al(III) complexes, the chloride ions are attached to the aluminum core. Structural details about these species were obtained by Saukkoriipi et al.,[36] who performed density functional theory (DFT) calculations in the gas and liquid phases. DFT and Hartree−Fock (HF) gas-phase calculations on aluminum chlorohydrate systems have also been reported by Pophristic et al.[37] Contrary to the common assumption that the Al coordination shell in these compounds consists only of OH groups and H_2O molecules, these calculations suggest that single Cl^- ion incorporation into the octahedral first hydration shells of the aluminum chlorohydrate monomer, dimer, and trimer increases the stability of these systems by ≥10 kcal/mol.

Several ion-pairing studies of monovalent and divalent metal (M) ions in interaction with chloride have been performed using conventional molecular dynamics (CMD) simulations based on two- and three-body interactions. For example, many theoretical studies have been reported for NaCl;[38−46] LiCl;[47] and alkaline-earth-metal−chloride solutions such as $MgCl^+$,[48] $CaCl^+$,[48−52] $SrCl^+$,[48,53,54] and $BaCl^+$.[48] Potential of mean force (PMF) calculations for these ion pairs have all been reported, and the computed structural, energetic, and thermodynamic properties have been compared with experimental and spectroscopic results. Whereas the association behavior between chloride and singly and doubly charged aqueous metal ions can be interpreted by CMD, similar analysis for highly charged metal ions is much less reliable. For these species, CMD methods are more difficult to apply because the many-body effects, such as the strong interactions of the highly charged ion center with the neighboring ligands, make the development of accurate interaction potentials (as used in CMD) extremely difficult.[55−65] These strong interactions are, however, essential to reliable predictions because they lead to significant alterations in both the hydrogen-bonding structure and the acid/base properties in the hydration region.

Ab initio molecular dynamics (AIMD) methods[66] provide a valuable means for treating highly charged ions in aqueous solutions.[60,61,64] Based on interactions calculated at the electronic-structure level as the simulation proceeds, these methods automatically take into account the valence electronic structure of the ions and solvating water molecules. They therefore incorporate the changes in interaction potential as a function of position in the hydration region that are necessary to obtain reliable predictions of the bonding in this region. Although such simulations provide a reliable parameter-free representation of the many-body interactions in the solution, this type of simulation is extremely time-consuming and requires a significant amount of computational resources. In our earlier works,[61,63,64,67−69] extensive Car−Parrinello-based MD (CPMD) simulations were performed showing the differences in the structure and dynamics of the water molecules in the hydration shells surrounding metal ions such as Fe^{3+} and Al^{3+} ions. Our results were found to be in agreement with the structural data obtained from X-ray scattering and EXAFS measurements.[70] In the present work, we performed CPMD simulations of an aqueous solution of $AlCl_3$ with the objective of investigating the ion-association behavior between chloride and aluminum. Al^{3+} is a closed-shell system, meaning that its total electronic structure can be represented with a restricted wave function. A series of CPMD simulations were performed for the aqueous $AlCl_3$ system by fixing the internuclear separation between the two ions at a certain value in each simulation. This allowed the free energy profile of the aluminum−chloride ion pair to be obtained. Thus, for the first time, the PMF of the Al^{3+}−Cl^- ion interaction, calculated at a high level of theory, is reported, and a detailed solvent structure analysis at different stages of the ion-pairing process is presented and compared to measured experimental data. X-ray diffraction data of aqueous solutions of $AlCl_3$ (1 and 2 M) were collected by Caminiti et al.,[71] who interpreted them using two models: one in which there is no correlation between the Al^{3+} and Cl^- solvating water molecules and a second in which the Cl^- ions have a hydration shell that is partially shared with the second hydration shell of Al^{3+}. The second model showed the best agreement between theoretical and experimental data. Our results are also compared to data from classical MD[56] and CPMD[57] theoretical studies of aqueous $AlCl_3$ solutions at concentrations of 0.28 and 0.8 M, respectively, that were reported in the literature. In both cases, the starting geometry of the simulation consisted of Cl^- anions separated from the Al^{3+} cation by two or more water molecules. No approach of one Cl^- ion to the hydrated Al^{3+} was apparent in these studies. However, such a dramatic change of solvation structure of the ions is expected to be a rare event and hardly observed within the time scale accessible by these simulations. For this reason, in this work, two additional CPMD simulations of an aqueous $AlCl_3$ solution were performed at 300 K with all three Cl^- ions unconstrained. These were initialized from contact ion pair (CIP) and solvent-separated ion pair (SSIP) starting configurations. We also performed CPMD simulations of a single Cl^- ion solvated with 64 water molecules to provide structural information about the systems at infinite dilution.

The article is organized as follows: In section 2, the computational methods used in this work are described. The results of constrained $AlCl_3$ CPMD simulations, a detailed analysis of solvent structure around the Al^{3+} and Cl^- ions, and a discussion of the electronic properties of solvating water molecules and Cl^- are presented in section 3. In section 4, we describe the results of the two unconstrained CPMD simulations of aqueous $AlCl_3$ solutions. Concluding remarks are given in section 5.

2. SIMULATION DETAILS

Car−Parrinello molecular dynamics simulations[66] of an aqueous $AlCl_3$ solution (containing Al^{3+} plus 3 Cl^- ions and 63 H_2O molecules) were performed within the framework of density functional theory (DFT)[72,73] plus generalized gradient (GGA) corrections (PBE96 exchange-correlation functional[74,75]) using the pseudopotential plane-wave program (NWPW module) contained in the NWChem computational chemistry package.[76] Although the inclusion of exact exchange is expected to improve the general accuracy of the PBE GGA approximation,[77−79] the cost of exact exchange is very high, and exchange was not included in this work because of the length of our CPMD simulations. We emphasize, however, that the use of the much more efficient DFT PBE formalism has been demonstrated to provide remarkably good results.[61,63,64,67−69,80−85] In addition, the energetics of the reactions we are considering are on the order of 10 kcal/mol, whereas the errors in DFT/GGA are estimated to be on the order of

kT or slightly larger. For example, the water dimer binding energy is estimated to be 5.3 kcal/mol for the PBE functional,[81] compared with the value of 5.2 kcal/mol measured experimentally.[86] The valence−core interaction was described by generalized norm-conserving Hamann pseudopotentials[87,88] modified into a separable form as suggested by Kleinman and Bylander.[89] For gradient-corrected calculations, the NWPW module automatically revises the pseudopotentials by generating them with the specified exchange-correlation functional. Because the original pseudopotential parametrizations suggested by Hamann produce stiff potentials, softer pseudopotentials were constructed by increasing the core radii, as follows: for H, r_{cs} = 0.8 au, r_{cp} = 0.8 au; for O, r_{cs} = 0.7 au, r_{cp} = 0.7 au, r_{cd} = 0.7 au; for Al, r_{cs} = 1.241 au, r_{cp} = 1.577 au, r_{cd} = 1.577 au; and for Cl, r_{cs} = 1.340 au, r_{cp} = 1.450 au, r_{cd} = 1.450 au. A nonlinear core correction[90] was also included for the Cl^- pseudopotential (semicore radius = 1.3 au, semicore charge = 0.279) to address the nonlinearity of the exchange-correlation energy. Valence orbitals were expanded in a plane-wave basis set with a wave function cutoff of 40 hartree and a density cutoff of 80 hartree. Periodic boundary conditions on the cubic simulation cell of side L = 12.414 Å (density near 1 g/cm^3) were applied; the Brillouin zone of the cell was sampled at the Γ point only. The Car−Parrinello equations of motion were integrated in the presence of Nosé−Hoover thermostats[91] at T = 300 K with a time step of 0.169 fs and a fictitious electron mass of 750 au. Although, in several previous molecular dynamics simulations,[83,92,93] the use of thermostats has been limited or avoided altogether in favor of collecting data in the microcanonical ensemble (constant E_{tot}) and controlling temperature by rescaling the ionic velocities, the canonical ensemble (constant NVT) was chosen here because the length of our simulations would have required a significant amount of velocity rescaling and quenching of the electronic degrees of freedom. To slow the OH bond dynamics, all hydrogen atoms were replaced by deuterium.

The simulations of the aqueous $AlCl_3$ solution were started from a configuration taken from prior molecular dynamics simulations[61] performed on an Al^{3+} ion solvated by 64 water molecules in a cubic box of side L = 12.414 Å. To generate an initial configuration, one first-shell water molecule was replaced by one Cl^- ion. Two additional Cl^- ions were then added to neutralize the net charge of the system. Our sample (Al^{3+} + 3Cl^- + 63H_2O) corresponds to an aqueous $AlCl_3$ solution at a concentration of 0.8 M. To initiate the simulations, the system was heated over a period of ∼6 ps. For equilibration, the temperature was increased in stages from 50 to 300 K (50 K/ps). The equilibrium distance between the Al^{3+} ion and the first-shell Cl^- ions was 2.3 Å. To compute the PMF, a series of constrained molecular dynamics simulations was performed using the SHAKE algorithm.[94] In this context, the internuclear separation between the two ions was fixed to a certain value in each simulation according to the expression

$$|r|^2 - r_{Al-Cl}{}^2 = 0 \quad (1)$$

where r is the instantaneous internuclear distance vector between ions Al^{3+} and Cl^- and r_{Al-Cl} is the constraint.

The Al^{3+}−Cl^- ion-pair distance was shortened from 2.3 to 1.9 Å, with intermediate step sizes of 0.1 Å, and elongated from 2.3 to 6.0 Å, with intermediate step sizes of 0.1 Å for r_{Al-Cl} in the interval of 2.3−3.0 Å and 0.2 Å for r_{Al-Cl} in the range of 3.0−6.0 Å. In total, 27 constrained CPMD simulations were performed at 300 K for 10−16 ps each. For each constrained simulation, the final position and velocities obtained after 1 ps of equilibration were used as the initial configuration for the next constraint value. The additional two chloride ions were allowed to move freely throughout the simulation cell. At each Al^{3+}−Cl^- separation, the mean force between the ion pair was calculated as

$$F(r) = \frac{1}{2}\langle r_u \cdot (F_{Al} - F_{Cl})\rangle \quad (2)$$

where r_u is a unit vector along the Al^{3+}−Cl^- direction and F_{Al} and F_{Cl} are the forces exerted on the ions Al^{3+} and Cl^-, respectively.

Each of them are the sum of the solvent force on the ion and the direct force between the solutes.[95] Statistics on the mean force were collected every 10 time steps over the CPMD simulation time of each constrained distance. Relatively long simulations (10−16 ps) were conducted for each interionic separation to ensure that the mean force has converged. Finally, the PMF between the aluminum, Al^{3+}, and chloride, Cl^-, ions, W_{Al-Cl}, was obtained by numerical integration of the mean force given by the relation

$$W_{Al-Cl}(r) = W(r_0) - \int_{r_0}^{r} F(r)\, dr \quad (3)$$

where r is the length of the constraint (fixed during each simulation). As a reference point, $W(r_0)$ was chosen as the free energy with the Cl^- in the bulk region separated by 6.0 Å from the Al^{3+} ion.

The solvent structure around the Al^{3+} and Cl^- ions was analyzed as a function of the constraint distance. The structure of the hydration shells of the Al^{3+} ion was determined by the analysis of the aluminum−oxygen radial distribution function, $g_{Al-O}(r)$, obtained from the results of the Al^{3+}−64-water-molecule CPMD simulation by Bylaska et al.[61] Thus, the constrained Cl^- ion was considered to be in the first hydration shell of Al^{3+} for r_{Al-Cl} values falling within the range 1.9−2.2 Å, whereas the range 3.6−4.6 Å was used for Cl^- residing in the second hydration shell of the cation. For $r_{Al-Cl} \geq$ 4.0 Å, many trajectories in which a water molecule was transferred from the second hydration shell or bulk solution to a contact position in the first hydration shell of the Al^{3+} ion were detected. In particular, for r_{Al-Cl} distances of 4.0, 4.2, 4.6, 4.8, 5.0, and 5.2 Å, a water exchange was observed during the simulation at ∼9.1, 2.0, 3.9, 3.5, 0.8, and 4.8 ps, respectively. One exception is the trajectory obtained at r_{Al-Cl} = 4.4 Å, in which no water transfer to the first hydration shell was detected for the 14 ps of our simulation. For r_{Al-Cl} = 5.4 Å, one water transfer between the second and first hydration shells of Al^{3+} occurred within the 1 ps of equilibration. Therefore, a first hydration shell of Al^{3+} composed of six water molecules was taken as the initial configuration for each constrained simulation with r_{Al-Cl} > 5.4 Å. Finally, we note that hydrolysis of first-shell water molecules occurred along three trajectories at r_{Al-Cl} = 3.2 Å (after 9.7 ps), 3.6 Å (from 12.6 to 12.8 ps and from 13.4 to 13.7 ps), and 3.8 Å (after 5.9 ps). Although the hydrolysis of aqueous Al^{3+} and its possible effect on Al^{3+}−Cl^- ion-pair formation might be an interesting topic in itself, it will not be discussed in this article because of the poor sampling of these species. Thus, the three trajectories for constraint distances of r_{Al-Cl} = 3.2, 3.6, and 3.8 Å were edited to remove the configurations containing the $Al(OH)^{2+}$ species to focus our analysis exclusively on Al^{3+}−Cl^- ion-pair formation in the absence of water ligand hydrolysis.

In this work, we also performed a CPMD simulation of a single Cl^- ion solvated with 64 water molecules (simulation cell of 12.414 Å) at 300 K for 22.4 ps, with 2.4 ps taken as equilibration. These simulations provided structural information about the systems at infinite dilution. Finally, we compared our results to a similar 12-ps CPMD simulation of 64 water molecules (no ions), which provided information about the bulk water structure. In addition, to further analyze the stability of the Al^{3+}−Cl^- CIP and SSIP, two simulations of an aqueous $AlCl_3$ solution were performed at 300 K with all three Cl^- ions unconstrained. These simulations were initialized from a starting configuration taken from our constrained simulations after 1 ps in which the separation between the Al^{3+} ion and one of the Cl^- ions was equal to 2.3 Å (corresponding to the CIP bond distance) and 6.0 Å (corresponding to the SSIP bond distance). In both cases, trajectories were collected for ∼17 ps.

Two gas-phase geometry optimizations of the $[Al(H_2O)_5Cl]^{2+}$ species were carried out at the DFT/PBE96 level of theory using the same plane-wave basis set as used in the CPMD simulations and using the local basis set 6-311G**.[96,97] The two computed gas-phase structure parameters were found to be in close agreement. The Al^{3+}−Cl^- bond distance of the optimized $[Al(H_2O)_5Cl]^{2+}$ complex under the plane-wave and local basis sets was 2.12 and 2.13 Å, respectively. The average bond length between the Al^{3+} cation and the first-shell water molecules was 1.99 Å for both the plane-wave and local basis sets, and the average first-shell water O−H distance was 0.96 and 0.98 Å, respectively.

3. RESULTS AND DISCUSSION OF THE CONSTRAINED CPMD SIMULATIONS

3.1. Potential of Mean Force. Figure 1 shows the average mean force values and the resulting PMF (or free energy difference profile) of the Al^{3+}−Cl^- ion pair with respect to the distance, r_{Al-Cl}, separating the two ions. For reference, we plotted the aluminum−oxygen radial distribution function, $g_{Al-O}(r)$, obtained from the results of the Al^{3+}−64-water-molecule CPMD simulation reported by Bylaska et al.[61] This $g_{Al-O}(r)$ distribution illustrates the spatial regions in which the constrained chloride ion is in the first and second hydration shells of the Al^{3+} ion defined by the first and second peaks, respectively, in $g_{Al-O}(r)$. Five characteristic points related to the local minima and barriers in the free energy profile between the Al^{3+} and Cl^- ions, labeled A−E, are identified in the figure. A pronounced global minimum (point A) assigned as a CIP is observed along the free energy path at a distance r_{Al-Cl} = 2.3 Å. This distance is 0.18 Å longer than the gas-phase species value of 2.12 Å. A free energy difference of −9.22 kcal/mol was found between this minimum and the reference point (point E) chosen with Cl^- in the bulk region separated by 6.0 Å from the Al^{3+} ion. This energy value is in agreement with the gas-phase estimate (at the HF level) of −10 kcal/mol of the stabilization energy of the aluminum chlorohydrate clusters reported by Pophristic et al.[37] When the Cl^- ion is moved from r_{Al-Cl} = 2.3 Å (point A) to r_{Al-Cl} = 3.6 Å (point B), a free energy barrier of 9.58 kcal/mol is encountered. This value is consistent with the free energy barriers reported for the Na^+−Cl^- (1.4 kcal/mol)[98] and Ca^{2+}−Cl^- (4.4 kcal/mol)[99] systems in that the dissociation barrier systematically increases with increasing charge of the central metal ion. Our free energy barrier height is roughly half the transition-state energy for an inner-sphere water-exchange reaction computed by Evans et al.[22] (21.4 kcal/mol), showing that the Al^{3+}−Cl^- bond is weaker than the Al^{3+}−inner-shell-water bond. The lifetime of the Cl^- anion in the first hydration shell of Al^{3+} can be estimated based on the free energy barrier value by using the Eyring equation.[100] It was found to be on the order of ∼1.5 μs, from which we estimated a corresponding Cl^- dissociation rate of ∼6.5 × 10^5 s^{-1}. Both of these quantities show that the dissociation of the bound chloride ion is expected to be much faster than the experimentally observed inner-sphere water-exchange reactions of a variety of aqueous aluminum complexes.[7,14] This suggests that the Al^{3+} and Cl^- ions might form a transient, short-lived contact ion pair, which might be difficult to detect. In Figure 1, two less pronounced local minima assigned as SSIPs were found at distances of r_{Al-Cl} = 4.4 Å (point C) and r_{Al-Cl} = 6.0 Å (point E). Interestingly, the minimum (point C) corresponds to the trajectory in which no water transfer to the first hydration shell of Al^{3+} is detected. The barrier (point D), at a distance of r_{Al-Cl} = 5.2 Å, between the two states is small (∼1 kcal/mol). Relative to $g_{Al-O}(r)$, the minima at points A and C correspond to regions of low concentration of waters of hydration, that is, between the first and second hydration shells of the Al^{3+} ion and between the second hydration shell and the bulk, respectively, whereas the minimum at point E is in the bulk region. The presence of these three minima is qualitatively in agreement with an Eigen−Wilkens mechanism.[101,102] In all CPMD trajectories, the two unconstrained Cl^- anions (labeled Cl_2 and Cl_3) are separated from the Al^{3+} cation by two or more water molecules (see the Supporting Information). The average distances from the Al^{3+} ion are 4.8 Å (Cl_2) and 6.6 Å (Cl_3), which coincide with the positions of local minima C and E.

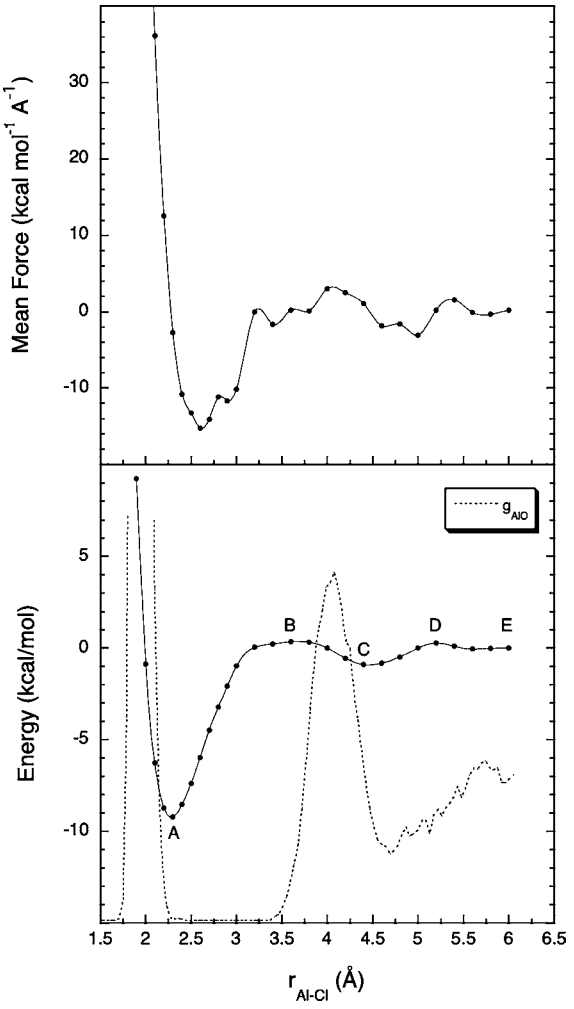

Figure 1. Average mean force values and the resulting potential of mean force (PMF, or free energy difference) of the Al^{3+}−Cl^- ion pair with respect to the distance separating the two ions, r_{Al-Cl}. The free energy difference was computed with respect to the free energy at r_{Al-Cl} = 6.0 Å. For reference, the aluminum−oxygen radial distribution function, $g_{Al-O}(r)$, obtained from the results of the Al^{3+}−64-water-molecule CPMD simulations reported by Bylaska et al.[61] is also plotted. The five points labeled A−E are characteristic of the formation of an ion pair.

3.2. Structural Analysis. Figure 2 provides a picture of the aluminum and chloride solvent structures with the density contours of the oxygen and hydrogen atoms at r_{Al-Cl} corresponding to the five characteristic points A−E. A corresponding snapshot is also shown on the right side of each plot (Cartesian coordinates are provided in the Supporting Information). The results indicate pronounced hydration shells and a rigid organization of the water molecules around the Al^{3+} ion, and the first hydration shell of the constrained Cl^- ion is found to be strongly influenced by the hydration-shell structure of the cation. As the Cl^- ion is moved from the first hydration shell of Al^{3+} to the bulk region, a well-ordered evolution of the first and second hydration shells of the aluminum ion is observed. In particular, at r_{Al-Cl} = 2.3 Å (point A), a well-defined octahedral arrangement of the first-hydration-shell water molecules around Al^{3+} with the Cl^- ion as part of the octahedron is clearly observed. This structure is

dx.doi.org/10.1021/ic301346k | Inorg. Chem. 2012, 51, 10856−10869

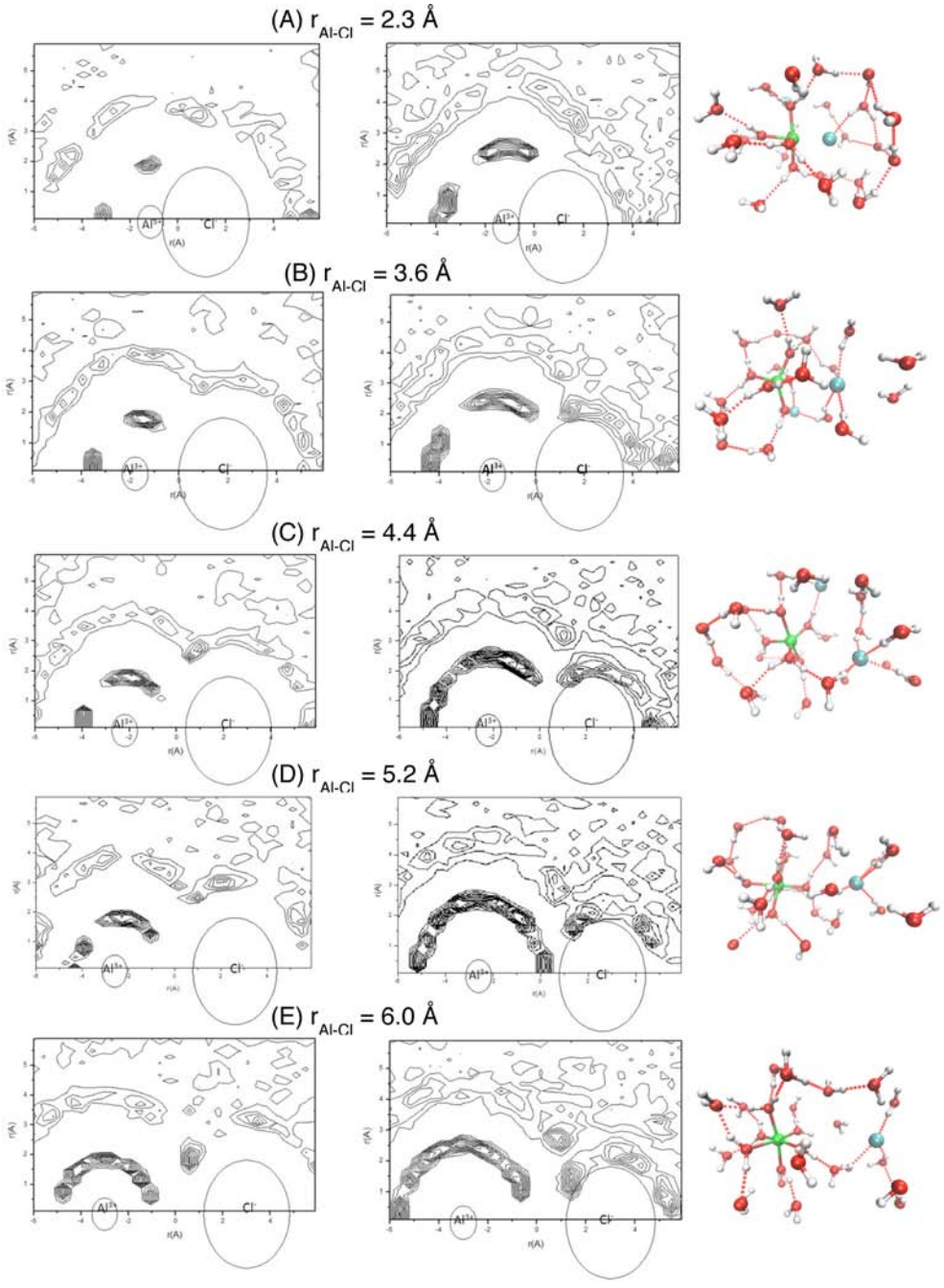

Figure 2. Aluminum−chloride association structures at 300 K revealed from the (left) oxygen and (right) hydrogen density contours obtained at r_{Al-Cl} = (A) 2.3, (B) 3.6, (C) 4.4, (D) 5.2, and (E) 6.0 Å. A corresponding snapshot is also shown on the right side of each plot.

maintained rigid as indicated by the density of the oxygen atoms being localized in nearly spherical contours. When the interionic separation is enlarged to the transition-state value (r_{Al-Cl} = 3.6 Å, point B), the first-shell octahedral structure around the cation is slightly disturbed. The contours of the density of the oxygen atoms near Al^{3+} begin spreading out, suggesting that the octahedral structure is less rigid. The hydration shell of the Cl^- ion is found to be particularly asymmetric, being partially composed of the first-shell water molecules of the aluminum ion. As the ion-pair distance increases (points C−E), the Cl^- ion passes through the second hydration shell of Al^{3+}, and the vacancy in the first hydration shell of Al^{3+} is progressively filled by a water molecule. At the same time, some hydrating water molecules from the first and second hydration shells of Al^{3+} start interacting directly with the chloride ion. In the case of the first-shell water molecules, the molecules generally point the negative end of their electric dipoles (their O atom) toward the Al^{3+} ion while making a H-bond with the Cl^- ion. At r_{Al-Cl} = 6.0 Å (point E), we clearly observe structures in which water molecules defined as bridging molecules are shared between the second shell of Al^{3+} and the first shell of Cl^-. These structures are found to be similar to the model used by Caminiti et al.[71] to interpret the X-ray diffraction data of a 2 M $AlCl_3$ aqueous solution. The results presented in Figure 2 show, however, essentially very small changes in the Al^{3+} average radial solvent structure. This would make it very difficult to discriminate between the CIP and SSIP species and could possibly explain why the $Al^{3+}Cl^-$ ion-pair

dx.doi.org/10.1021/ic301346k | Inorg. Chem. 2012, 51, 10856−10869

species has not been detected experimentally yet. To interpret in more detail the $Al^{3+}-Cl^-$ PMF in terms of the hydration-shell water structure, a detailed analysis of solvent structure around both Al^{3+} and Cl^- ions is presented next.

3.2.1. Aluminum Ion. Very similar aluminum−oxygen radial distribution functions were found for all constrained CPMD simulations with two well-defined and isolated peaks in the ranges of 1.84−1.90 and 3.95−4.07 Å for the first and second peaks, respectively (see the Supporting Information). These confirm pronounced hydration shells and a rigid organization of the water molecules around the cation and are in agreement with the Al^{3+}−64-water-molecule CPMD simulation data,[61] which display two maxima at 1.91 and 4.06 Å. We observe that the first $Al^{3+}-O$ peak height and width vary slightly as the Al^{3+} and Cl^- ions are separated as a result of the replacement of the Cl^- anion, initially located in the first hydration shell of Al^{3+}, by a water molecule. As mentioned above, this replacement does not occur until the ion-pair distance is quite long (≥4.0 Å). It is thus evident that the average radial structure, $g_{Al-O}(r,)$ is not strongly affected by the position of the Cl^- ion. This makes it very difficult to discriminate between the CIP and SSIP species using radial structures derived from experimental diffraction techniques. The molecular orientations of the hydration water molecules near the cation, however, change as the ion-pair separation is increased. To characterize these changes, structural parameters from the first and second hydration shells of Al^{3+} as a function of the distance between the Al^{3+} and Cl^- ions were computed.

First Hydration Shell of Al^{3+}. The average first-shell oxygen coordination number (CN_I) and the average first-shell $Al-O_I$ bond distance calculated for each constrained value of r_{Al-Cl} are presented in Figure 3. Figure 4 shows the distribution of $O_I-Al^{3+}-O_I$ angles within the first shell of the Al^{3+} ion obtained from constrained simulations A−E. Generally, an octahedral first hydration shell leads to a distribution of O_I-Al-O_I angles with two well-defined peaks at 90° and 180°, whereas the presence of an additional peak at 120° reveals a trigonal-bipyramidal first hydration shell.

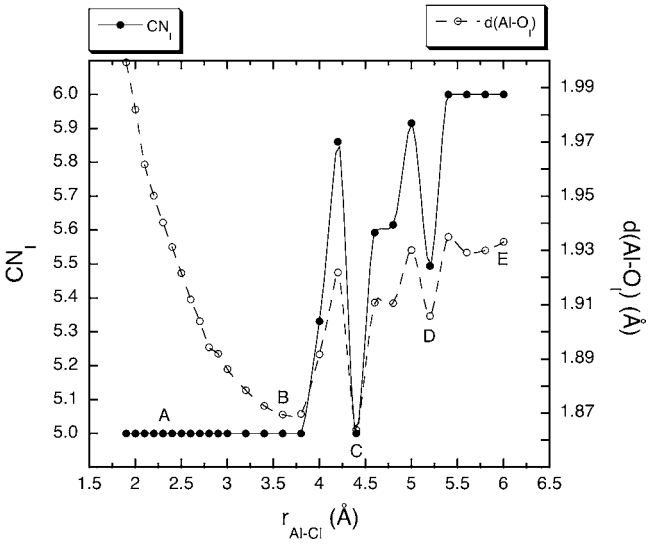

Figure 3. Average first-shell oxygen coordination number (CN_I) and average first-shell $Al-O_I$ bond distance from constrained CPMD simulations as a function of the internuclear separation between the Al^{3+} and Cl^- ions.

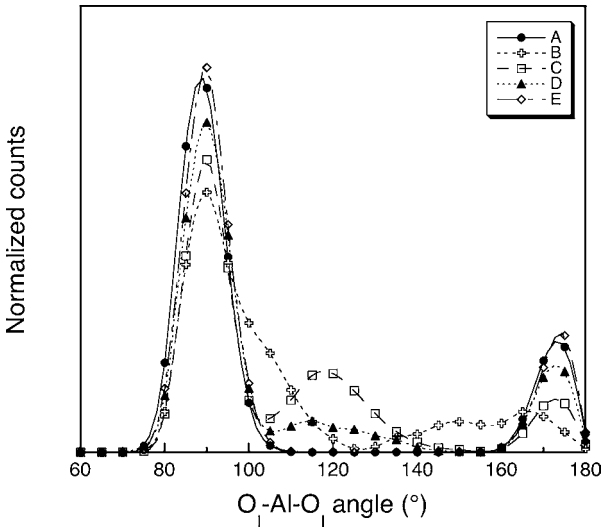

Figure 4. Distribution of $O_I-Al^{3+}-O_I$ angles within the first hydration shell of the Al^{3+} ion obtained for the characteristic simulations A−E corresponding to r_{Al-Cl} = (A) 2.3, (B) 3.6, (C) 4.4, (D) 5.2, and (E) 6.0 Å.

At r_{Al-Cl} = 2.3 Å (point A), the Cl^- ion is bound to the Al^{3+} ion, forming a structure that corresponds to $[Al(H_2O)_5Cl]^{2+}$ with CN_I = 5. The average $Al-O_I$ bond distance in this simulation is 1.94 Å, in agreement with the previously published gas-phase geometrical parameter of the monomer $Al(H_2O)_6Cl_3$ in a structure in which one chloride ion is bound to the Al^{3+} ion.[37] It is also consistent with the gas-phase distance that we obtained for the $[Al(H_2O)_5Cl]^{2+}$ complex. Compared to the results obtained from previous unconstrained CPMD simulation of $AlCl_3$[57] aqueous solution in a SSIP configuration (1.92 Å), the average $Al-O_I$ bond distance appears to be slightly longer, indicating weaker Al^{3+}−first-shell-water interactions. This labilizing effect is due to the partial screening of the Al^{3+} charge by the Cl^- ion in the first hydration shell of the cation. The $O_I-Al^{3+}-O_I$ angle distribution for constrained simulation A, illustrated in Figure 4, exhibits two large peaks at 90° and 175°, indicating that the Al^{3+} ion is coordinating the five water molecules in an octahedral arrangement with the Cl^- ion as part of the octahedron, as clearly illustrated in Figure 2A. When r_{Al-Cl} is changed from 2.3 to 3.6 Å (point B), the chloride ion crosses the interface between the first and second hydration shells of Al^{3+} and the CN_I does not change. The $Al-O_I$ bond distance decreases from 1.94 to 1.87 Å. The distribution of $O_I-Al^{3+}-O_I$ angles corresponding to constrained simulation B presents a first peak centered at exactly 90° and a second located at 165°, showing that the first hydration shell of Al^{3+} for this ion-pair bond length has octahedral symmetry. The fact that the two peaks are considerably broadened into intermediate angles, however, suggests that the octahedral structure has become less rigid around Al^{3+}. As mentioned before, this can been seen in Figure 2B, in which the contour of the density of the first-shell oxygen atoms is spread out. For 3.6 Å < r_{Al-Cl} ≤ 4.6 Å, the chloride ion is in the second hydration shell of Al^{3+}, and water molecules begin to fill the vacancy in the first hydration shell created by the removal of the Cl^- ion. Water transfers were observed in the simulations with r_{Al-Cl} fixed at 4.0, 4.2, and 4.6 Å after 9.1, 2.0, and 3.9 ps, respectively. For these constrained simulations, the average CN_I vlue was found to be greater than

dx.doi.org/10.1021/ic301346k | Inorg. Chem. 2012, 51, 10856−10869

5 (equal to 5.3, 5.9, and 5.6, respectively), and the Al−O_I distance increases by up to 0.05 Å. For r_{Al-Cl} = 4.4 Å (point C), no water transfer to the first shell was observed, and the CN_I value remained equal to 5. The corresponding average Al−O_I bond distance was found to be 1.86 Å. At this constraint, the loss of octahedral symmetry of the first hydration shell of Al^{3+} is evident mainly through the O_I−Al−O_I angle distribution given in Figure 4 (curve C). In addition to the peaks at 90° and 175°, a broad peak is now formed at 120°, indicating that the first hydration shell of Al^{3+} undergoes a transformation from an octahedral to a trigonal-bipyramidal symmetry. Finally, for r_{Al-Cl} > 4.6 Å, the constrained Cl^- ion reaches the bulk region, and a first hydration shell of Al^{3+} containing six water molecules is readily formed. We note that, in simulation D (r_{Al-Cl} = 5.2 Å), the water transfer after 4.8 ps results in an average CN_I value of 5.5 and an average Al−O_I distance of 1.91 Å. The O_I−Al−O_I distribution for constrained simulation D shows two well-formed peaks at 90° and 175° and a very broad peak at 115°, which reflects the mixing of a trigonal-bipyramidal and octahedral first-shell symmetry of the cation. At r_{Al-Cl} = 6.0 Å (point E), the average CN_I value is 6, and the average Al−O_I distance is 1.93 Å, indicating the formation of an octahedral $[Al(H_2O)_6]^{3+}$ hexaqua species. A clear return to octahedral symmetry is also confirmed by the O_I−Al−O_I distribution (Figure 4, curve E), which displays two well-formed peaks at 90° and 175°. These results are in agreement with the structural data obtained from the analysis of X-ray measurements.[71] They also compare very well with the theoretical results of the unconstrained CPMD simulations of Al^{3+} [61] and $AlCl_3$[57] aqueous solutions.

Second Hydration Shell of Al^{3+}. For all r_{Al-Cl} constraint values, the H-bonding between the first and second hydration shells of the Al^{3+} ion was found to be primarily a trigonal H-bond network in which each first-shell water donor coordinates two second-shell water molecules. This result is consistent with the analysis of X-ray diffraction experiments[71] and predictions of the unconstrained CPMD simulations of Al^{3+} [61] and $AlCl_3$[57] aqueous solutions and shows that the hydration structure is dominated by the Al^{3+} ion. However, when the constrained Cl^- anion resides in the second hydration shell of the Al^{3+} ion, small amounts of tetrahedral coordination (i.e., a first-shell water acceptor and donor coordinating water molecules in the second hydration shell) are also observed in which acceptor bonds make up to ∼4% of the total first−second-shell H-bond coordination.

The average second-shell oxygen coordination number (CN_{II}) of Al^{3+} and the average second-shell Al−O_{II} distance, for each r_{Al-Cl} constraint, are given in Figure 5. We observe that the presence of the Cl^- ion at r_{Al-Cl} = 2.3 Å (point A) results in the formation of a second hydration shell containing on average ∼10 water molecules. The resulting Al−O_{II} bond distance is equal to 4.09 Å. Compared to the results obtained from unconstrained CPMD simulation of $AlCl_3$[57] aqueous solution, CN_{II} decreased by ∼2 beause of the replacement of a first-shell water molecule by a Cl^- ion. When r_{Al-Cl} is increased from 2.3 to 3.6 Å (point B), the chloride ion approaches the second shell of Al^{3+}, which decreases the number of water molecules in the second shell by ∼0.5, as the Al−O_{II} bond distance undergoes a contraction from 4.09 to 3.96 Å. This can be explained by the fact that the larger separation between the Al^{3+} and Cl^- ions increases the charge in the first hydration region, strengthening the interaction with the second hydration shell. For r_{Al-Cl} > 3.6 Å, as the Cl^- ion crosses the second hydration shell and enters

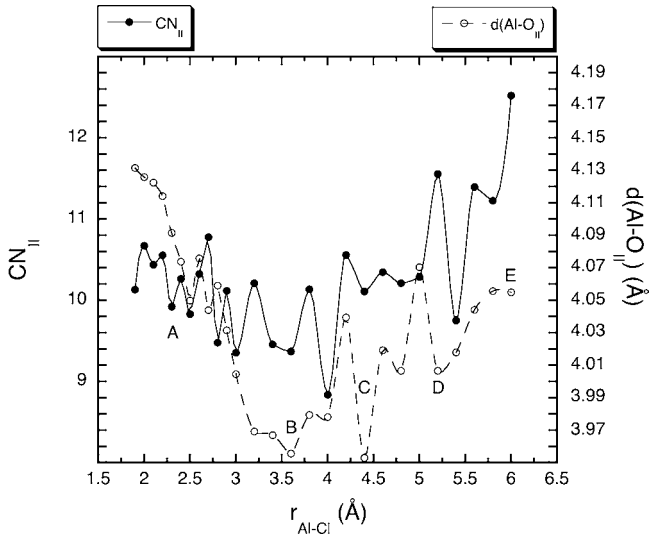

Figure 5. Average second-shell oxygen coordination number (CN_{II}) and average second-shell Al−O_{II} bond distance from constrained AIMD simulations of an aqueous $AlCl_3$ solution as a function of the internuclear separation between the Al^{3+} and Cl^- ions.

the bulk region, the vacancy in the second hydration shell of Al^{3+} is filled by two bulk water molecules, and the CN_{II} reaches ∼12. The average Al−O_{II} bond distance clearly increases to 4.05 Å. These results are consistent with the structural data obtained from X-ray measurements.[71] They are also in very good agreement from the results of the unconstrained CPMD simulations of Al^{3+} [61] and $AlCl_3$[57] aqueous solutions. We note that, upon placing the Cl^- ion at r_{Al-Cl} = 4.4 Å, which corresponds to constrained simulation C, in which no water transfer was observed, leads to an average CN_{II} value of 10.1. The corresponding average Al−O_{II} bond distance was found to be equal to a value of 3.95 Å.

3.2.2. Chloride Ion. The chloride−oxygen radial distribution functions show, for each CPMD constraint simulation, a maximum in the approximate range of 3.07−3.13 Å (see the Supporting Information). This range is consistent with the Cl^-−64-water-molecule CPMD simulation data that we obtained, which display a maximum at 3.09 Å. For constrained simulation A, a second small peak was also observed at r_{Cl-O} = 4.25 Å. This feature comes from the first-hydration-shell oxygen atoms of the Al^{3+} ion. Contrary to the aluminum−oxygen radial distribution function, which displays two very well-defined hydration shells, $g_{Cl-O}(r)$ is not as easily interpreted. Indeed, although the radial distribution function shows a maximum for each constraint simulation, there is no clear first minimum that would indicate a highly structured Cl^- first hydration shell. Therefore, to determine average structure parameters for the Cl^- ion, a water molecule was defined to be in the first hydration shell of the anion if the distance between the chloride ion and the oxygen atom was ≤3.80 Å, as determined from the chloride−oxygen radial distribution function obtained from the results of our Cl^-−64-water-molecule CPMD simulation. This cutoff distance is in agreement with the values reported for Cl^- in water by Heuft et al.[103] and Mallik et al.[104] The calculated average CN value of Cl^- based on a Cl^-−O cutoff distance equal to 3.80 Å varies from a value of ∼8−9 associated with r_{Al-Cl} < 3.6 Å to ∼6−7 at r_{Al-Cl} ≥ 3.6 Å (see the Supporting Information). This latter CN value agrees with the value calculated from our Cl^-−64-water-molecule CPMD simulation

dx.doi.org/10.1021/ic301346k | Inorg. Chem. 2012, 51, 10856−10869

(6.6) and is in agreement with the experimental CN value of 6[105] and the values reported by Tongraar et al.[106] and Heuft et al.[103] As illustrated in Figure 2, the large CN value of Cl^- for $r_{Al-Cl} < 3.6$ Å is due to the first-shell water molecules of the aluminum ion that partially compose the hydration shell of the Cl^- ion. However, if one considers the number of water molecules that, in addition to being within the first shell of Cl^-, form a $Cl^-\cdots H-O$ angle of $\geq 140°$ and, as a result, coordinate the Cl^- ion with a H-bond, we see that most of the first-shell water molecules of the aluminum ion cannot coordinate the Cl^- with a H-bond since they are strongly coordinated to the Al^{3+} ion. When the Cl^- ion enters the second hydration shell of the Al^{3+} ion ($r_{Al-Cl} \geq 3.6$ Å), the CN value of Cl^- begins to decrease, and the number of water molecules that coordinate the anion with a H-bond increases (see the Supporting Information). Only as the Cl^- ion leaves the second shell of Al^{3+} to enter into the bulk region ($r_{Al-Cl} > 4.6$ Å), the two numbers of water molecules tend to converge, showing that the water molecules in the first hydration shell of Cl^- are now free to coordinate the chloride ion and form a H-bond.

Is the solvation shell of dissociated Cl^- ion asymmetric, as was previously interpreted?[57] To characterize the symmetry of the hydration shell of the Cl^- ion, we calculated the vector $\vec{R}_{cage}$ that, as already introduced by Ikeda et al.,[57] is given by the equation

$$\vec{R}_{cage} = \sum (\vec{R}_{O_i} - \vec{R}_{Cl}) \quad (4)$$

where the sum for the oxygen positions, $\vec{R}_{O_i}$, is taken over the oxygen atoms in the instantaneous hydration shell of the chloride ion located at $\vec{R}_{Cl}$.

Figure 6 (solid line) shows the magnitude of the vector $\vec{R}_{cage}$ calculated for the constrained Cl^- ion as a function of r_{Al-Cl}.

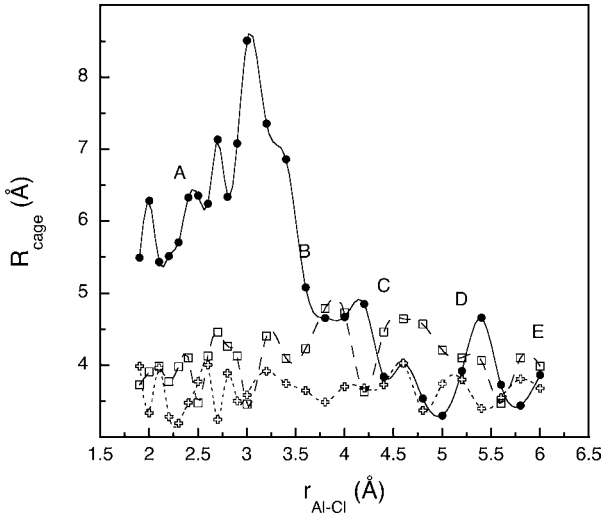

Figure 6. Magnitude of the vector $\vec{R}_{cage}$ calculated for the constrained (solid line) and unconstrained (dotted lines) Cl^- ions as a function of the separation r_{Al-Cl} between Al^{3+} and the constrained Cl^- ion.

The values obtained for the two unconstrained Cl^- ions are also compared (dotted lines, open symbols). At $r_{Al-Cl} < 3.6$ Å, the magnitude of $\vec{R}_{cage}$ for the constrained Cl^- ion is substantial, on average, equal to 6.48 ± 0.43 Å. This suggests that the hydration shell of the anion is strongly asymmetric because of the influence of the first-shell water molecules of the aluminum ion. However, when the Cl^- ion approaches the second hydration shell of Al^{3+}, the magnitude of the $\vec{R}_{cage}$ vector decreases rapidly. For $r_{Al-Cl} \geq 3.6$ Å, $\vec{R}_{cage}$ reaches an average value of 4.12 ± 0.29 Å, similar to the values obtained for the two unconstrained chloride ions (3.65 ± 0.12 and 4.11 ± 0.18 Å). These latter values are in agreement with the value obtained from our Cl^-−64-water-molecule CPMD simulation (3.97 ± 1.85 Å). They also agree with the published value of 3.32 Å for $AlCl_3$ solution[57] and the interpretation of a mostly asymmetric solvation shell of dissociated Cl^-.

3.2.3. Aluminum Chloride Association. To study in more detail the correlation between the hydration shell of Cl^- and its separation relative to the Al^{3+} ion, the number of water molecules shared between the two hydrated ions was analyzed. In Figure 7, the total numbers of water molecules in the first hydration shell of Cl^- shared with the Al^{3+} first shell, second shell, and the bulk region are illustrated as a function of the distance r_{Al-Cl} (solid line). The numbers of water molecules coordinating the Cl^- ion with a H-bond are also given (dotted line). We note that, to do this estimation, we had to limit our analysis to a single image of the simulation cell centered on the Al^{3+} ion. Because of this, the number of coordinating water molecules for large distances might not sum to the actual coordination number. The data presented in Figure 7 facilitate a revealing interpretation of the presence of minima along the PMF reported in Figure 1. In particular, the deep minimum (point A) corresponds to a configuration in which the Cl^- ion is poorly H-bond-coordinated to first- and second-shell water molecules and thus is primarily due to the direct electrostatic interaction between the anion and the Al^{3+} cation. Going from minimum A to transition state B, the constrained Cl^- ion crosses the interface between the first and second hydration shells of Al^{3+}, and the number of second-shell water molecules that coordinate the Cl^- ion with a H-bond increases on average from 0.4 to 1.0 as the number of H-bonds between Cl^- and the bulk water molecules increases from 0.8 to 3. This process requires a free energy difference corresponding to the barrier observed in Figure 1. At $r_{Al-Cl} = 4.4$ Å in constrained simulation C, a pentacoordinate $[Al(H_2O)_5]^{3+}$ species displaying a geometry significantly different from the octahedral species was found to be quite stable. The five first-hydration-shell water molecules of Al^{3+} undergo a transformation, which proceeds favorably, from an octahedral to a nearly trigonal-bipyramidal symmetry with no H-bond with the Cl^- ion. This result is consistent with the analysis of ^{17}O nuclear magnetic resonance experiments[18] and predictions of the unconstrained CPMD simulations of $AlOH^{2+}$ [18] aqueous solution. Finally, for $r_{Al-Cl} >$ 4.6 Å (points D and E), the Al^{3+} first hydration shell has returned to a fully formed six-coordinate octahedral symmetry, and the vacancy in the second hydration shell is filled. In minimum E, a total of six to seven water molecules coordinating the Cl^- ion coming from the second hydration shell of Al^{3+} and the bulk are observed, constituting an ideal H-bonding environment for both the cation and the anion. A comparison between the solid and dotted curves in Figure 7a,b demonstrates the significant structural influence of the Al^{3+} ion on the H-bonding network. Until the Cl^- ion passes through the second hydration shell of Al^{3+}, large disparities between the solid and dotted curves are observed. The water molecules in the first and second hydration shells of Al^{3+} cannot coordinate the Cl^- ion with a H-bond because they are preferentially oriented to coordinate the highly charged Al^{3+} ion. When the Cl^- ion leaves the second hydration shell to enter into the bulk region, the two curves in Figure 7a,b tend to converge, showing

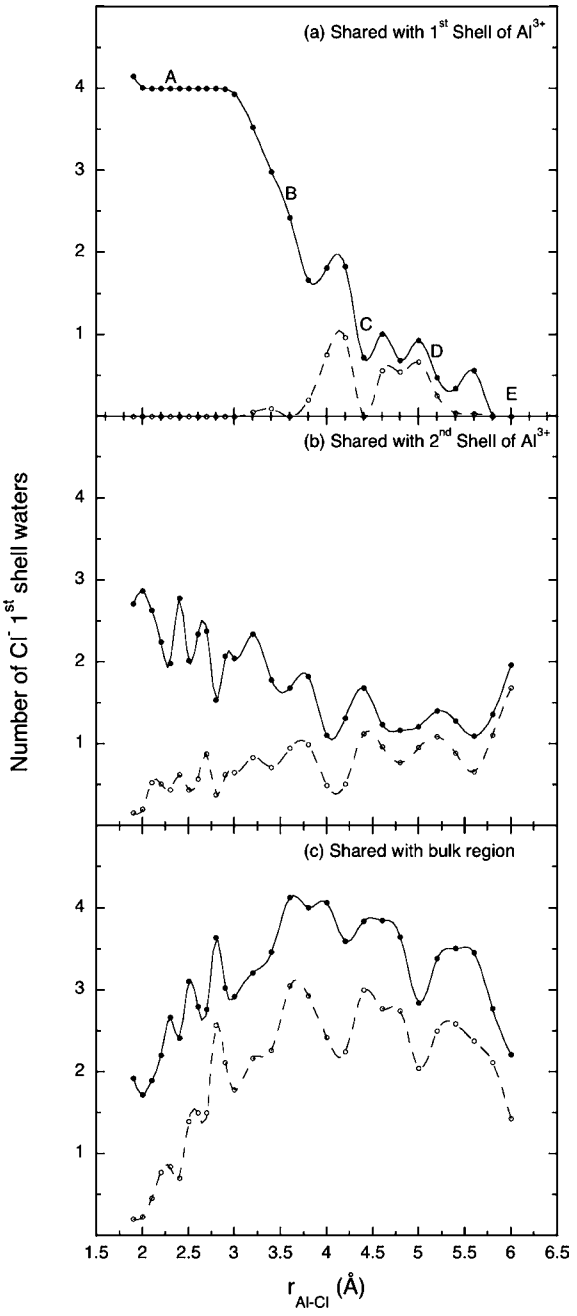

Figure 7. Number of water molecules in the first hydration shell of Cl^- (solid line) shared with the (a) first and (b) second shells of the Al^{3+} ion and the (c) bulk region. The number of water molecules that, in addition to being within the first shell of Cl^-, form a Cl···H−O angle greater than or equal to 140° and coordinate the Cl^- ion with a H-bond is also plotted (dotted line).

that the Cl^- ion is now positioned so that the water molecules in the first and second hydration shells can coordinate the Cl^- and Al^{3+} ions at the same time. For shared bulk water molecules (Figure 7c), there is a strong similarity between the solid and dotted curves for all r_{Al-Cl} values; the water molecules in this region are less rigidly stuck around the cation and generally H-bond with the anion. The results presented in Figure 7 summarize main characteristics of the solvent structure around both the Al^{3+} and Cl^- ions discussed above. They support the idea of strongly pronounced hydration shells and a rigid organization of the water molecules around the Al^{3+} cation with a small influence from the Cl^- anion. This can explain how difficult it could be to discriminate between the CIP and SSIP species. Again, this could possibly explain why the $Al^{3+}-Cl^-$ ion-pair species has not yet been detected experimentally.

3.3. Electronic Structure. An important feature of the CPMD method used in this work is the first-principles evaluation of the electronic structure of the system in the instantaneous structure of the fluid. In these simulations, changes in the electronic structure were investigated by calculating the polarization of the system using the method of maximally localized Wannier functions.[107−110] This approach assigns dipole moments to individual atoms or molecules in a condensed phase by assuming that the electronic charge is distributed as point charges located on the Wannier function centers (WFCs).[111,112] The dipole moment of the water molecules in the first and second hydration shells of Al^{3+} and the bulk and the dipole moment of the Cl^- ion were calculated as a function of the separation of the Al^{3+} and Cl^- ions. A total of 165 conformations of the aqueous $AlCl_3$ system were used, including at least five distinct sampled conformations for each individual constraint. For some constraints (r_{Al-Cl} = 4.0, 4.2, 4.6, 4.8, 5.0, and 5.2 Å), because the Al^{3+} cation existed as both five- and six-coordinated complexes, a total of 10 configurations were sampled with five configurations for each coordination state. This distinction was made so that differences in polarization between the five- and six-coordinated Al^{3+} complexes could be observed. Finally, a Wannier analysis was performed on five configurations from the Cl^-−64-water-molecule CPMD simulation so that a standard could be established for Cl^- polarization in pure water.

3.3.1. Solvating Water Molecules of Al^{3+}. The dipole moments of the solvating water molecules in the first (diamond) and second (square) hydration shells of Al^{3+} and bulk (triangle) are plotted in Figure 8. The solid and open symbols provide the values of the dipole moment for the five- and six-coordinated Al^{3+} complexes, respectively. At r_{Al-Cl} = 1.9 Å, when the Cl^- ion is constrained to be in the first hydration

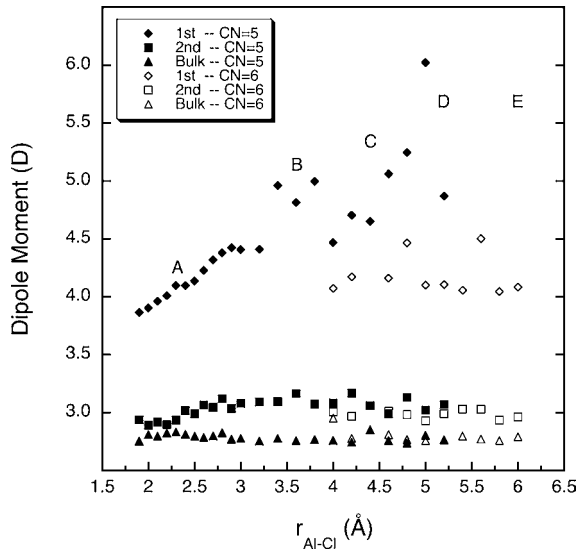

Figure 8. Dipole moments of the water molecules in the first (diamonds) and second (squares) hydration shells of Al^{3+} and in the bulk (triangles), calculated as a function of the separation r_{Al-Cl} between the Al^{3+} and Cl^- ions. The solid and open symbols are for five- and six-coordinated Al^{3+} complexes, respectively.

dx.doi.org/10.1021/ic301346k | Inorg. Chem. 2012, 51, 10856−10869

shell of Al^{3+}, the average dipole moment of the five water molecules in the octahedral coordination shell is 3.9 ± 0.4 D. This value should be compared to the theoretical value of 4.1 ± 0.2 D obtained from the Al^{3+}−64-water-molecule CPMD simulation.[64] The small decrease of the dipole moment of the water molecules is in response to the charge of the Al^{3+} ion being partially screened by Cl^-. As the Cl^- ion is moved beyond the first shell, the calculated dipole moment of the five first-shell water molecules increases with an average value of 4.8 ± 1.9 D at r_{Al-Cl} = 3.6 Å (point B). For r_{Al-Cl} > 3.6 Å, as the Cl^- ion crosses the second hydration shell and enters the bulk region, the five first-shell water molecules, which are still in a nearly trigonal-bipyramid arrangement around the cation, display a very large average dipole moment. A maximum average value of 6.0 ± 3.6 D is obtained at r_{Al-Cl} = 5.0 Å. However, when the vacancy in the first hydration shell of Al^{3+} is filled, the dipole moments of the six first-hydration-shell water molecules, which have returned to an octahedral arrangement around the cation, are much less polarized. They have a dipole moment equal, on average, to 4.2 ± 2.6 D. These results are very important because they illustrate the major changes that occur in the first hydration region of Al^{3+} as the ion-pair separation is increased. At r_{Al-Cl} = 6.0 Å, when the Cl^- ion is in the bulk region, the six first-shell water molecules have an average dipole moment of 4.1 ± 0.3 D. This value agrees well with the value of 4.1 ± 0.2 D obtained from the Al^{3+}−64-water-molecule CPMD simulation.[64]

In all constrained simulations, second-shell and bulk water molecules have average dipole moments equal to 3.0 ± 1.5 and 2.8 ± 2.2 D, respectively, for the five-coordinated Al^{3+} complexes and 3.0 ± 0.9 and 2.8 ± 2.3 D, respectively, for the six-coordinated Al^{3+} complexes. All are similar to the value of 3.1 ± 0.1 D obtained for pure bulk water.[64] This result supports the idea that there is little direct influence of the chloride ion on the dipole moment of the water molecules, as previously suggested in the literature,[62,65,103,113,114] and that the Al^{3+} cation−water interactions are dominant in determining the polarization state of the $AlCl_3$ solution.

3.3.2. Chloride Ion. When the Cl^- ion is constrained to be in the first hydration shell of the Al^{3+}, a strong dipole moment of the anion is created essentially by interaction with the Al^{3+} cation (see the Supporting Information). At r_{Al-Cl} = 1.9 Å, the average value of the anion dipole moment is 3.0 ± 0.3 D. As the anion is transferred from the first shell to the second shell of the Al^{3+} ion, the dipole moment of the Cl^- ion strongly decreases from about ∼3 D to ∼0.5 D. When the Cl^- ion is in the second shell of the Al^{3+} ion and in the bulk region, that is, separated by at least 3.6 Å from the Al^{3+} ion, the average dipole moment is 0.7 ± 0.8 and 0.9 ± 1.1 D for the five- and six-coordinated Al^{3+} complexes, respectively. These dipole moments are consistent with the calculated values for the two unconstrained chloride ions (0.7 ± 1.6 and 0.9 ± 2.0 D) and the value of 0.9 ± 0.3 D obtained from the results of our Cl^-−64-water-molecule CPMD simulation. These values are also in agreement with the values of 0.7 ± 0.3 and 0.5 ± 0.2 D reported by Ikeda et al.[57] and Zhao et al.,[65] respectively, and with extensive CPMD studies of chloride ion.[62,115]

To correlate the values of the Cl^- dipole moment with the local environment of the anion, the orientation of the dipole moment relative to, first, its hydration shell and, second, the aluminum ion was calculated. Two angles, θ and ϕ, were defined as the angles between the dipole moment $\vec{\mu}$ of Cl^- and the two vectors $\vec{R}_{Al-Cl}$ and $\vec{R}_{cage}$, respectively. The distributions of the average angles θ and ϕ as a function of the r_{Al-Cl} distance are shown in Figure 9 in terms of cos θ and cos ϕ. Also plotted

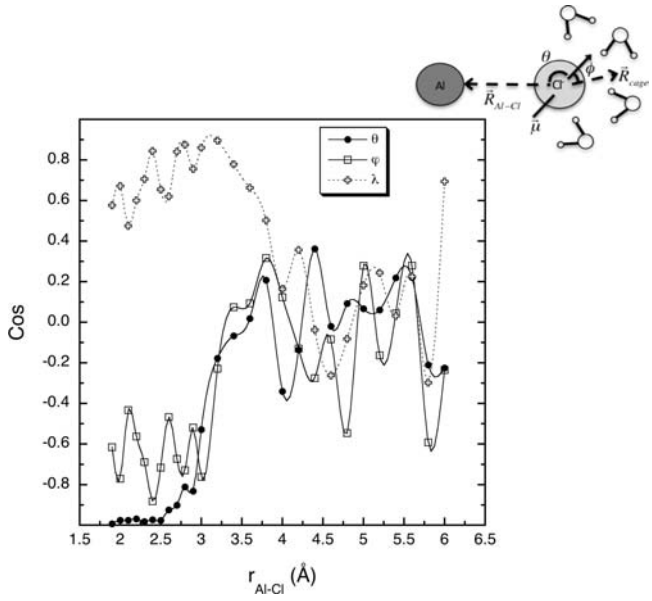

Figure 9. Distributions of cos θ and cos ϕ as a function of the r_{Al-Cl} distance. The angles θ and ϕ are defined as the angles between the dipole moment $\vec{\mu}$ of Cl^- and the two distinct vectors $\vec{R}_{Al-Cl}$ and $\vec{R}_{cage}$, respectively (see inset). The vector $\vec{R}_{Al-Cl}$ is defined as $\vec{R}_{Al} - \vec{R}_{Cl}$, whereas $\vec{R}_{cage}$ is given by eq 4. Also plotted is cos λ, where λ is defined as the angle between $\vec{R}_{Al-Cl}$ and $\vec{R}_{cage}$.

is cos λ, where λ is the angle between $\vec{R}_{Al-Cl}$ and $\vec{R}_{cage}$. For r_{Al-Cl} ≤ 3.6 Å, the vector $\vec{R}_{cage}$ is mostly defined by the first-shell water molecules of Al^{3+} favoring an orientation parallel to the vector $\vec{R}_{Al-Cl}$ (cos $\lambda \approx 1$). In these simulations, the strong dipole moment of the anion is created essentially by interaction with the Al^{3+} cation. The average angles of 138° and 122° for θ and ϕ, respectively, show that the dipole vector points away from the Al^{3+} ion, thus orienting the Cl^- electrons simultaneously toward the Al^{3+} cation and toward the solvent cage. As the Cl^- ion crosses the second hydration shell and enters the bulk region, the distributions of the angles θ, ϕ, and λ display large fluctuations around the axis of cos θ (or cos ϕ or cos λ) = 0. For r_{Al-Cl} > 3.6 Å, the average angle θ is 89° (cos θ = 0.02 ± 1.62), and the average angle ϕ is equal to 95° (cos ϕ = −0.08 ± 1.88). The two vectors $\vec{R}_{Al-Cl}$ and $\vec{R}_{cage}$ form an average angle of 82° (cos λ = 0.14 ± 1.63). At r_{Al-Cl} = 6.0 Å, the average values obtained for cos θ and cos ϕ are −0.23 ± 0.62 and −0.23 ± 0.66, respectively. This latter value is in close agreement with the average value of cos ϕ = −0.35 reported by Ikeda et al.[57] These results demonstrate that the induced net dipole moment of Cl^- is no longer associated with the aluminum ion but with the formation of the solvation shell of the Cl^- itself.

4. RESULTS AND DISCUSSION OF THE UNCONSTRAINED CPMD SIMULATIONS

We performed two unconstrained CPMD simulations for 17 ps each, identified in this section as CIP and SSIP simulations, starting from configurations taken from the constrained simulations in which distances of 2.3 and 6.0 Å, respectively, separated the Al^{3+} ion and one of the Cl^- ions (labeled Cl_1). In both starting configurations, the two other Cl^- anions (labeled

dx.doi.org/10.1021/ic301346k | Inorg. Chem. 2012, 51, 10856−10869

Cl_2 and Cl_3) are separated from the Al^{3+} cation by two or more water molecules. Figure 10 provides the aluminum−oxygen,

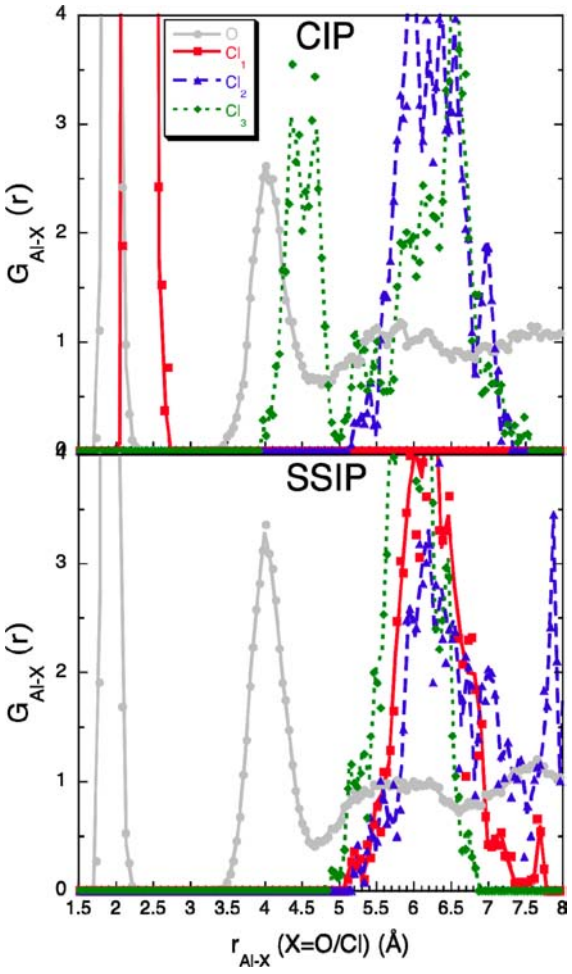

Figure 10. Aluminum−oxygen and individual aluminum−chloride radial distribution functions, $g_{Al-X}(r)$ with X = O, Cl_1, Cl_2 and Cl_3, from unconstrained contact ion pair (CIP) and solvent-separated ion pair (SSIP) CPMD simulations of the aqueous $AlCl_3$ solution.

$g_{Al-O}(r)$, and individual aluminum−chloride, $g_{Al-X}(r)$ with X = Cl_1, Cl_2, and Cl_3, radial distribution functions obtained from the results of the CIP and SSIP simulations. The $g_{Al-O}(r)$ radial distribution functions of CIP and SSIP both show the presence of two well-defined peaks, revealing the first and second hydration shells of the cation. As a result of the presence of Cl_1 in the first hydration shell of Al^{3+}, the peak heights of the CIP simulation are smaller than those of the SSIP simulation. In $g_{Al-Cl1}(r)$ computed for the CIP simulation, the single peak located at 2.3 Å shows that the Cl_1^- anion, which initially coordinates the Al^{3+} cation, remains in this coordination state for the entire 17 ps of the CPMD simulation. The corresponding function obtained from the SSIP simulation has a peak at a distance equal to 6.2 Å, very close to the initial separation of 6.0 Å. Thus, relatively minor changes in the position of the Cl_1 ion are observed. For the CIP and SSIP simulations, both of the two solvent-separated Cl^- ions, Cl_2 and Cl_3, occupy the bulk region, as demonstrated by the two large peaks of the corresponding radial distribution function, $g_{Al-Cl}(r)$, in the wide range of 5.0−7.5 Å. Exceptions include one Cl^- anion (Cl_3) in the CIP simulation, which was initially present in the second hydration shell of Al^{3+} and remained in this coordination state for roughly 4 ps before moving to larger Al−Cl distances for the remaining 13 ps. This configuration, however, was not observed to have an effect on the Cl_1 position. Also, in our SSIP simulation, the Cl_2 ion, initially located at 6 Å from the Al^{3+} ion, fluctuated to larger distances (up to 8 Å) for ∼5 ps before returning to 7 Å.

The structural parameters from the first and second hydration shells of Al^{3+} were computed for the CIP and SSIP simulations (see the Supporting Information). The results show that the structure around the cation from the unconstrained CIP and SSIP simulations very closely resembles that found for the constrained simulations from which their initial configurations were taken. The analysis of the first hydration shell of each chloride ion obtained from the CIP and SSIP simulations also agrees with what we observed for the constrained simulations. The coordination number, defined as the number of oxygen atoms closer than 3.8 Å to the Cl^- ion, was found to be equal to ∼6−7, except for Cl_1 from the CIP simulation, for which it was equal to 9 as a consequence of the presence of the Al^{3+} first-shell water molecules. The number of shared H-bonded water molecules between the Al^{3+} and Cl^- ions closely agrees with the values reported in Figure 7. This shows that the structures obtained from the various constrained CPMD simulations are well-equilibrated in the global (CIP) and local (SSIP) free energy minima.

5. CONCLUSIONS

The ion-pairing behavior between chloride and aluminum in an aqueous $AlCl_3$ solution containing 63 water molecules was studied by means of constrained CPMD simulations at 300 K in which the r_{Al-Cl} distance between the Al^{3+} ion and a single Cl^- ion was fixed. The calculated PMF of the aluminum−chloride ion pair shows a pronounced minimum at a distance of r_{Al-Cl} = 2.3 Å, suggesting the formation of a CIP. When the Cl^- ion is moved from 2.3 Å to 3.6 Å (when the Cl^- ion reaches the second hydration shell of the Al^{3+} ion), a free energy barrier of 9.58 kcal/mol is observed. The existence of two local minima assigned as SSIPs was established at distances of r_{Al-Cl} = 4.4 and 6.0 Å. The activation barrier between these distances was found to be small (∼1 kcal/mol). The positions of the minima identified along the free energy path show that the Cl^- ion is inclined to reside in regions with low concentrations of water molecules, that is, at the boundaries between the first and second shells of the Al^{3+} ion and the second shell and the bulk. Detailed analyses of solvent structure around the Al^{3+} and Cl^- ions over the simulated results indicate (1) pronounced hydration shells and a rigid organization of the water molecules around the Al^{3+} ion and (2) a significant structural influence of the Al^{3+} ion on the H-bonding network and hence on the first hydration shell of the constrained Cl^- ion. The deep free energy minimum relative to the association of Al^{3+} and Cl^- ions (CIP) corresponds to a configuration in which the Cl^- ion is poorly H-bond-coordinated to first- and second-shell water molecules of the Al^{3+} ion and is primarily due to the direct electrostatic interaction between the anion and the Al^{3+} cation. Until the Cl^- ion passes through the second hydration shell of Al^{3+}, the water molecules lying in the first or second hydration shells of Al^{3+} cannot coordinate the Cl^- ion with a H-bond because they are preferentially oriented to coordinate the highly charged Al^{3+} ion. Only as the Cl^- ion leaves the second hydration shell to enter into the bulk region are the water molecules of the first and second hydration shells oriented so

dx.doi.org/10.1021/ic301346k | Inorg. Chem. 2012, 51, 10856−10869

that they can coordinate the Cl^- and Al^{3+} ions at the same time, constituting an ideal H-bonding environment for both the cation and the anion.

The electronic structure of the system was investigated as a function of the separation of the Al^{3+} and Cl^- ions using the method of maximally localized Wannier functions. The calculations demonstrated the strong polarization of the water molecules in the first hydration shell of Al^{3+}. Major changes in the first hydration region of Al^{3+} can result from the removal of a Cl^- ion from the first hydration shell of the cation. In all constrained simulations, we found that both second-shell and bulk water molecules have a dipole moment similar to the value obtained for pure bulk water. In addition, we calculated, for each constraint, the induced net dipole moment of the Cl^- ion. An important feature is the decrease of the dipole moment when the Cl^- ion is transferred from the first shell to the second shell of the Al^{3+} ion. As the Cl^- ion is in the second shell of the Al^{3+} ion and in the bulk region, the average dipole moment is consistent with the calculated values for the unconstrained chloride ions.

Finally, we performed two unconstrained simulations of aqueous $AlCl_3$ solution at 300 K from starting configurations in which distances equal to 2.3 Å (CIP) and 6.0 Å (SSIP) separated the Al^{3+} ion and one of the Cl^- ions. The results show that both the starting configurations of the CIP and SSIP simulations are stable over the 17 ps of CPMD simulations. The structures from the unconstrained CIP and SSIP simulations very closely resemble those found in the constrained simulations from which their initial configurations were taken, confirming their stability.

■ ASSOCIATED CONTENT

Ⓢ Supporting Information

Average $Al^{3+}-Cl^-$ distances of the three Cl^- ions from all constrained CPMD simulations of the aqueous $AlCl_3$ solution. Aluminum−oxygen and chloride−oxygen radial distribution functions obtained for the constrained CPMD simulations (A−E). Coordination number of the constrained Cl^- ion, number of water H-bonds coordinating the Cl^- ion, and dipole moment of the constrained Cl^- ion calculated as a function of the separation r_{Al-Cl} between the Al^{3+} and Cl^- ions. Average parameters of the first and second hydration shells of the Al^{3+} ion from unconstrained contact ion pair (CIP) and solvent-separated ion pair (SSIP) CPMD simulations of the aqueous $AlCl_3$ solution. Cartesian coordinates of the snapshots of the constrained CPMD simulations A−E shown in Figure 2. This material is available free of charge via the Internet at http://pubs.acs.org.

■ AUTHOR INFORMATION

Corresponding Author

*E-mail: ecauet@ulb.ac.be.

Present Addresses

[‡]Université Libre de Bruxelles, CPi160/09, 50 Avenue F. D. Roosevelt, B-1050 Brussels, Belgium.

[⊥]Vrije Universiteit Brussel, 2 Pleinlaan, B-1050 Brussels, Belgium.

Author Contributions

[§]These authors contributed equally.

Notes

The authors declare no competing financial interest.

■ ACKNOWLEDGMENTS

This work was supported by the U.S. Department of Energy's Office of Basic Energy Sciences, Division of Chemical Sciences, Geosciences and Biosciences (Grant DE-FG02-10ER1 6126). Some of the calculations were performed on the Chinook computing system at the EMSL, a national scientific user facility sponsored by the Department of Energy's Office of Biological and Environmental Research and located at Pacific Northwest National Laboratory. Pacific Northwest National Laboratory is operated by Battelle Memorial Institute. We also thank the Scientific Computing Staff, Office of Energy Research, and the U.S. Department of Energy for a grant of computer time at the National Energy Research Scientific Computing Center, Berkeley, CA. E.C. thanks the Belgian American Educational Foundation (BAEF) for a postdoctoral fellowship and the FRS-FNRS (Fonds National de la Recherche Scientifique de Belgique). Finally, we thank Ying Chen for his kind help in the preparation of Figure 2.

■ REFERENCES

(1) Smith, R. W. *Coord. Chem. Rev.* **1996**, *149*, 81.
(2) Baes, C. F. J.; Mesmer, R. E. *Hydrolysis of Cations*; Wiley: New York, 1976.
(3) Akitt, J. W.; Farthing, A. *J. Chem. Soc., Dalton Trans.* **1981**, 1624.
(4) Brown, P. L.; Sylva, R. N.; Batley, G. E.; Ellis, J. *J. Chem. Soc., Dalton Trans.* **1985**, 1967.
(5) Singhal, A.; Keefer, K. D. *J. Mater. Res.* **1994**, *9*, 1973.
(6) Allouche, L.; Gérardin, C.; Loiseau, T.; Férey, G.; Taulelle, F. *Angew. Chem., Int. Ed.* **2000**, *39*, 511.
(7) Casey, W. H. *Chem. Rev.* **2006**, *106*, 1.
(8) Fournier, A. C.; Shafran, K. L.; Perry, C. C. *Anal. Chim. Acta* **2008**, *607*, 61.
(9) Sipos, P. *J. Mol. Liq.* **2009**, *146*, 1.
(10) Bogatko, S.; Geerlings, P. *Phys. Chem. Chem. Phys.* **2012**, *14*, 8058.
(11) Phillips, B. L.; Casey, W. H.; Neugebauer-Crawford, S. *Geochim. Cosmochim. Acta* **1997**, *61*, 3041.
(12) Phillips, B. L.; Casey, W. H.; Karlsson, M. *Nature* **2000**, *404*, 379.
(13) Casey, W. H.; Phillips, B. L.; Karlsson, M.; Nordin, S.; Nordin, J. P.; Sullivan, D. J.; Neugebauer-Crawford, S. *Geochim. Cosmochim. Acta* **2000**, *64*, 2951.
(14) Casey, W. H.; Phillips, B. L. *Geochim. Cosmochim. Acta* **2001**, *65*, 705.
(15) Lee, A. P.; Phillips, B. L.; Casey, W. H. *Geochim. Cosmochim. Acta* **2002**, *66*, 577.
(16) Phillips, B. L.; Lee, A.; Casey, W. H. *Geochim. Cosmochim. Acta* **2003**, *67*, 2725.
(17) Casey, W. H.; Swaddle, T. W. *Rev. Geophys.* **2003**, *41*, 1008.
(18) Swaddle, T. W.; Rosenqvist, J.; Yu, P.; Bylaska, E. J.; Phillips, B. L.; Casey, W. H. *Science* **2005**, *308*, 1450.
(19) Phillips, B. L.; Tossell, J. A.; Casey, W. H. *Environ. Sci. Technol.* **1998**, *32*, 2865.
(20) Rustad, J. R. *Rev. Mineral. Geochem.* **2001**, *42*, 169.
(21) Wang, J.; Rustad, J. R.; Casey, W. H. *Inorg. Chem.* **2007**, *46*, 2962.
(22) Evans, R. J.; Rustad, J. R.; Casey, W. H. *J. Phys. Chem. A* **2008**, *112*, 4125.
(23) Bogatko, S.; Moens, J.; Geerlings, P. *J. Phys. Chem. A* **2010**, *114*, 7791.
(24) Yu, P.; Phillips, B. L.; Casey, W. H. *Inorg. Chem.* **2001**, *40*, 4750.
(25) Bogatko, S.; Cauët, E.; Geerlings, P. *J. Phys. Chem. C* **2011**, *115*, 6910.
(26) Sillén, L. G.; Martell, A. E. *Stability Constants of Metal-Ion Complexes*; Special Publication 17; Chemical Society: London, 1964. Sillén, L. G.; Martell, A. E. *Stability Constants of Metal-Ion Complexes*; Special Publication 25; Chemical Society: London, 1971.

(27) Perrin, D. D. *Stability Constants of Metal-Ion Complexes*; Pergamon Press: Oxford, U.K., 1979; Part B: Organic Ligands.
(28) Högfeldt, E. *Stability Constants of Metal-Ion Complexes*; Pergamon Press: Oxford, U.K., 1982; Part A: Inorganic Ligands.
(29) Hefter, G. *Pure Appl. Chem.* **2006**, *78*, 1571.
(30) Marcus, Y.; Hefter, G. *Chem. Rev.* **2006**, *106*, 4585.
(31) Näslund, L. A.; Cavalleri, M.; Ogasawara, H.; Nilsson, A.; Pettersson, L. G. M.; Wernet, P.; Edwards, D. C.; Sandstrom, M.; Myneni, S. *J. Phys. Chem. A* **2003**, *107*, 6869.
(32) Diaz-Moreno, S.; Munoz-Paez, A.; Martinez, J. M.; Pappalardo, R. R.; Sanchez Marcos, E. *J. Am. Chem. Soc.* **1996**, *118*, 12654.
(33) Sarpola, A.; Hietapelto, V.; Jalonen, J.; Jokela, J.; Laitinen, R. S. *J. Mass Spectrom.* **2004**, *39*, 423.
(34) Sarpola, A.; Hietapelto, V.; Jalonen, J.; Jokela, J.; Laitinen, R. S.; Rämö, J. *J. Mass Spectrom.* **2004**, *39*, 1209.
(35) Hellman, H.; Laitinen, R. S.; Kaila, L.; Jalonen, J.; Hietapelto, V.; Jokela, J.; Sarpola, A.; Rämö, J. *J. Mass Spectrom.* **2006**, *41*, 1421.
(36) Saukkoriipi, J.; Sillanpää, A.; Laasonen, K. *Phys. Chem. Chem. Phys.* **2005**, *7*, 3785.
(37) Pophristic, V.; Klein, M. L.; Holerca, M. N. *J. Phys. Chem. A* **2004**, *108*, 113.
(38) Guàrdia, E.; Rey, R.; Padró, J. A. *Chem. Phys.* **1991**, *155*, 187.
(39) Rey, R.; Guardia, E. *J. Phys. Chem.* **1992**, *96*, 4712.
(40) Dang, L. X. *J. Chem. Phys.* **1992**, *97*, 1919.
(41) Smith, D. E.; Dang, L. X. *J. Chem. Phys.* **1994**, *100*, 3757.
(42) Chialvo, A. A.; Cummings, P. T.; Cochran, H. D.; Simonson, J. M.; Mesmer, R. E. *J. Chem. Phys.* **1995**, *103*, 9379.
(43) Chialvo, A. A.; Cummings, P. T.; Simonson, J. M.; Mesmer, R. E. *J. Chem. Phys.* **1996**, *105*, 9248.
(44) Chialvo, A. A.; Cummings, P. T.; Simonson, J. M.; Mesmer, R. E. *J. Mol. Liq.* **1997**, *73*, 361.
(45) Sherman, D. M.; Collings, M. D. *Geochem. Trans.* **2002**, *3*, 102.
(46) Chialvo, A. A.; Simonson, J. M. *J. Chem. Phys.* **2003**, *118*, 7921.
(47) Zhang, Z.; Duan, Z. *Chem. Phys.* **2004**, *297*, 221.
(48) Larentzos, J. P.; Criscenti, L. J. *J. Phys. Chem. B* **2008**, *112*, 14243.
(49) Guàrdia, E.; Robinson, A.; Padró, J. A. *J. Chem. Phys.* **1993**, *99*, 4229.
(50) Dang, L. X.; Smith, D. E. *J. Chem. Phys.* **1995**, *102*, 3483.
(51) Guàrdia, E.; Padró, J. A. *J. Chem. Phys.* **1995**, *102*, 3485.
(52) Chialvo, A. A.; Simonson, J. M. *J. Chem. Phys.* **2003**, *119*, 8052.
(53) Smith, D. E.; Dang, L. X. *Chem. Phys. Lett.* **1994**, *230*, 209.
(54) Seward, T. M.; Henderson, C. M. B.; Charnock, J. M.; Driesner, T. *Geochim. Cosmochim. Acta* **1999**, *63*, 2409.
(55) Wasserman, E.; Rustad, J. R.; Xantheas, S. S. *J. Chem. Phys.* **1997**, *106*, 9769.
(56) Lauenstein, A.; Hermansson, K.; Lindgren, J.; Probst, M.; Bopp, P. A. *Int. J. Quantum Chem.* **2000**, *80*, 892.
(57) Ikeda, T.; Hirata, M.; Kimura, T. *J. Chem. Phys.* **2003**, *119*, 12386.
(58) Spangberg, D.; Hermansson, K. *J. Chem. Phys.* **2004**, *120*, 4829.
(59) Ikeda, T.; Hirata, M.; Kimura, T. *J. Chem. Phys.* **2006**, *124*, 074503.
(60) Ikeda, T.; Boero, M.; Terakura, K. *J. Chem. Phys.* **2007**, *127*, 07403.
(61) Bylaska, E. J.; Valiev, M.; Rustad, J. R.; Weare, J. H. *J. Chem. Phys.* **2007**, *126*, 104505.
(62) Guàrdia, E.; Skarmoutsos, I.; Masia, M. *J. Chem. Theory Comput.* **2009**, *5*, 1449.
(63) Cauët, E.; Bogatko, S. A.; Weare, J. H.; Fulton, J. L.; Schenter, G.; Bylaska, E. J. *J. Chem. Phys.* **2010**, *132*, 194502.
(64) Bogatko, S. A.; Bylaska, E. J.; Weare, J. H. *J. Phys. Chem. A* **2010**, *114*, 2189.
(65) Zhao, Z.; Rogers, D. M.; Beck, T. L. *J. Chem. Phys.* **2010**, *132*, 014502.
(66) Car, R.; Parrinello, M. *Phys. Rev. Lett.* **1985**, *55*, 2471.
(67) Atta-Fynn, R.; Bylaska, E. J.; Schenter, G.; de Jong, W. A. *J. Phys. Chem. A* **2011**, *115*, 4665.
(68) Atta-Fynn, R.; Johnson, D. F.; Bylaska, E. J.; Ilton, E. S.; Schenter, G.; de Jong, W. A. *Inorg. Chem.* **2012**, *51*, 3016.
(69) Bogatko, S.; Cauët, E.; Bylaska, E. J.; Schenter, G.; Fulton, J. L.; Weare, J. H., manuscript submitted.
(70) Fulton, J. L.; Bylaska, E. J.; Bogatko, S.; Balasubramanian, M.; Cauët, E.; Schenter, G.; Weare, J. H. *J. Phys. Chem. Lett.* **2012**, DOI: 10.1021/jz3008497.
(71) Caminiti, R.; Licheri, G.; Piccaluga, G.; Pinna, G.; Radnai, T. *J. Chem. Phys.* **1979**, *71*, 2473.
(72) Hosenberg, P.; Kohn, W. *Phys. Rev. B* **1964**, *136*, 864.
(73) Kohn, W.; Sham, L. J. *Phys. Rev. A* **1965**, *140*, 1133A.
(74) Perdew, J. P.; Burke, K.; Ernzerhof, M. *Phys. Rev. Lett.* **1996**, *77*, 3865.
(75) Perdew, J. P.; Burke, K.; Ernzerhof, M. *Phys. Rev. Lett.* **1997**, *78*, 1396.
(76) Valiev, M.; Bylaska, E. J.; Govind, N.; Kowalski, K.; Straatsma, T. P.; van Dam, H. J. J.; Wang, D.; Nieplocha, J.; Apra, E.; Windus, T. L.; de Jong, W. A. *Comput. Phys. Commun.* **2010**, *181*, 1477.
(77) Yoo, S.; Zeng, X. C.; Xantheas, S. S. *J. Chem. Phys.* **2009**, *130*, 221102.
(78) Schmidt, J.; VandeVondele, J.; Kuo, I. F. W.; Sebastiani, D.; Siepmann, J. I.; Hutter, J.; Mundy, C. J. *J. Phys. Chem. B* **2009**, *113*, 11959.
(79) Yoo, S.; Xantheas, S. S. *J. Chem. Phys.* **2011**, *134*, 121105.
(80) Schwegler, E.; Galli, G.; Gygi, F. *Phys. Rev. Lett.* **2000**, *84*, 2429.
(81) Grossman, J. C.; Schwegler, E.; Draeger, E. W.; Gygi, F.; Galli, G. *J. Chem. Phys.* **2004**, *120*, 300.
(82) VandeVondele, J.; Mohamed, F.; Krack, M.; Hutter, J.; Sprik, M.; Parrinello, M. *J. Chem. Phys.* **2005**, *122*, 014515.
(83) White, J. A.; Schwegler, E.; Galli, G.; Gygi, F. *J. Chem. Phys.* **2000**, *113*, 4668.
(84) Lightstone, F. C.; Schwegler, E.; Hood, R. Q.; Gygi, F.; Galli, G. *Chem. Phys. Lett.* **2001**, *343*, 549.
(85) Lightstone, F. C.; Schwegler, E.; Allesch, M.; Gygi, F.; Galli, G. *ChemPhysChem* **2005**, *6*, 1745.
(86) Curtiss, L. A.; Frurip, D. J.; Blander, M. *J. Chem. Phys.* **1979**, *71*, 2703.
(87) Hamann, D. R.; Schluter, M.; Chiang, C. *Phys. Rev. Lett.* **1979**, *43*, 1494.
(88) Hamann, D. R. *Phys. Rev. B* **1989**, *40*, 2980.
(89) Kleinman, L.; Bylander, D. M. *Phys. Rev. Lett.* **1982**, *48*, 1425.
(90) Louie, S. G.; Froyen, S.; Cohen, M. L. *Phys. Rev. B* **1982**, *26*, 1738.
(91) Nose, S. *J. Chem. Phys.* **1984**, *81*, 511.
(92) Sprik, M.; Hutter, J.; Parrinello, M. *J. Chem. Phys.* **1996**, *105*, 1142.
(93) Lyubartsev, A. P.; Laasonen, K.; Laaksonen, A. *J. Chem. Phys.* **2001**, *114*, 3120.
(94) Ryckaert, J. P.; Ciccotti, G.; Berendsen, H. J. C. *J. Comput. Phys.* **1977**, *23*, 327.
(95) Ciccotti, G.; Ferrario, M.; Hynes, J. T.; Kapral, R. *Chem. Phys.* **1989**, *129*, 241.
(96) McLean, A. D.; Chandler, G. S. *J. Chem. Phys.* **1980**, *72*, 5639.
(97) Krishnan, R.; Binkley, J. S.; Seeger, R.; Pople, J. A. *J. Chem. Phys.* **1980**, *72*, 650.
(98) Timko, J.; Bucher, D.; Kuyucak, S. *J. Chem. Phys.* **2010**, *132*, 114510.
(99) Timko, J.; De Castro, A.; Kuyucak, S. *J. Chem. Phys.* **2011**, *134*, 204510.
(100) Eyring, H. *J. Chem. Phys.* **1935**, *3*, 107.
(101) Richens, D. T. *The Chemistry of Aqua Ions*; John Wiley & Sons, 1997.
(102) Richens, D. T. *Chem. Rev.* **2005**, *105*, 1961.
(103) Heuft, J. M.; Meijer, E. J. *J. Chem. Phys.* **2003**, *119*, 11788.
(104) Mallik, B. S.; Semparithi, A.; Chandra, A. *J. Chem. Phys.* **2008**, *129*, 194512.
(105) Bergström, P.-A.; Lindgren, J.; Kristiansson, O. *J. Phys. Chem.* **1991**, *95*, 8575.

(106) Tongraar, A.; Rode, B. M. *Phys. Chem. Chem. Phys.* **2002**, *5*, 357.
(107) Wannier, G. H. *Phys. Rev.* **1937**, *52*, 0191.
(108) Foster, J. M.; Boys, S. F. *Rev. Mod. Phys.* **1960**, *32*, 300.
(109) Silvestrelli, P. L.; Marzari, N.; Vanderbilt, D.; Parrinello, M. *Solid State Commun.* **1998**, *107*, 7.
(110) Berghold, G.; Mundy, C. J.; Romero, A. H.; Hutter, J.; Parrinello, M. *Phys. Rev. B* **2000**, *61*, 10040.
(111) Vanderbilt, D.; Kingsmith, R. D. *Phys. Rev. B* **1993**, *48*, 4442.
(112) Marzari, N.; Vanderbilt, D. *Phys. Rev. B* **1997**, *56*, 12847.
(113) Krekeler, C.; Hess, B.; Delle Site, L. *J. Chem. Phys.* **2006**, *125*, 054305.
(114) Krekeler, C.; Delle Site, L. *J. Phys.: Condens. Matter* **2007**, *19*, 192101.
(115) Masia, M. *J. Chem. Phys.* **2008**, *128*, 184107.